Clinical Cancer Research

WNT/β-catenin Pathway Activation Correlates with Immune Exclusion across Human Cancers

Jason J. Luke[1], Riyue Bao[2,3], Randy F. Sweis[1], Stefani Spranger[4], and Thomas F. Gajewski[1,4]

Abstract

Purpose: The T-cell-inflamed phenotype correlates with efficacy of immune-checkpoint blockade, whereas non-T-cell-inflamed tumors infrequently benefit. Tumor-intrinsic WNT/β-catenin signaling mediates immune exclusion in melanoma, but association with the non-T-cell-inflamed tumor microenvironment in other tumor types is not well understood.

Experimental Design: Using The Cancer Genome Atlas (TCGA), a T-cell-inflamed gene expression signature segregated samples within tumor types. Activation of WNT/β-catenin signaling was inferred using three approaches: somatic mutations or somatic copy number alterations (SCNA) in β-catenin signaling elements including *CTNNB1, APC, APC2, AXIN1*, and *AXIN2*; pathway prediction from RNA-sequencing gene expression; and inverse correlation of β-catenin protein levels with the T-cell-inflamed gene expression signature.

Results: Across TCGA, 3,137/9,244 (33.9%) tumors were non-T-cell-inflamed, whereas 3,161/9,244 (34.2%) were T-cell-inflamed. Non-T-cell-inflamed tumors demonstrated significantly lower expression of T-cell inflammation genes relative to matched normal tissue, arguing for loss of a natural immune phenotype. Mutations of β-catenin signaling molecules in non-T-cell-inflamed tumors were enriched three-fold relative to T-cell-inflamed tumors. Across 31 tumors, 28 (90%) demonstrated activated β-catenin signaling in the non-T-cell-inflamed subset by at least one method. This included target molecule expression from somatic mutations and/or SCNAs of β-catenin signaling elements (19 tumors, 61%), pathway analysis (14 tumors, 45%), and increased β-catenin protein levels (20 tumors, 65%).

Conclusions: Activation of tumor-intrinsic WNT/β-catenin signaling is enriched in non-T-cell-inflamed tumors. These data provide a strong rationale for development of pharmacologic inhibitors of this pathway with the aim of restoring immune cell infiltration and augmenting immunotherapy.

See related commentary by Dangaj et al., p. 2943

Introduction

Immunotherapies targeting immune checkpoints have contributed to a marked improvement in treatment outcomes in patients with advanced cancer. In melanoma, anti-cytotoxic T lymphocyte antigen 4 (CTLA-4) and anti-programmed death 1 (PD-1) antibodies have demonstrated robust response rates with years of durability in some patients (1, 2) and improvement in overall survival (3, 4). Significant clinical activity of PD-1-targeting agents has led to FDA approval in multiple additional cancer entities. Despite this broad activity, only a subset of patients benefits from treatment within each cancer subtype, and molecular mechanisms to explain primary resistance in these patients remain incompletely understood.

High expression of specific immune cell genes in the tumor microenvironment, described as the T-cell-inflamed phenotype, has been observed to correlate with response to multiple immunotherapies including therapeutic vaccines and checkpoint blocking antibodies (1, 5–10). Conversely, the non-T-cell-inflamed tumor microenvironment appears to closely associate with lack of clinical benefit to immunotherapy, particularly with anti-PD-1 antibodies (9, 10). Categorization of tumors using transcriptional profiles marking the T-cell-inflamed gene expression signature is advantageous as it can define biologically relevant patient subpopulations and set a framework in which to investigate hypothetical mechanisms for primary immunotherapy resistance.

Although multiple molecular mechanisms could theoretically disfavor a T-cell-inflamed microenvironment, several lines of investigation have indicated that specific oncogenic molecular aberrations can be sufficient to drive this immune exclusion phenotype in some cases. Tumor cell–intrinsic WNT/β-catenin signaling in melanoma was the first somatic alteration associated with the non-T-cell-inflamed tumor microenvironment in patients, and was demonstrated to be causal using a genetically-engineered mouse model (11). The mechanism of this effect appears to be through transcriptional repression of key chemokine genes that leads to lack of Batf3-lineage dendritic cell recruitment and subsequent failure to prime and recruit $CD8^+$ T cells (11, 12). This effect is dominant in the tumor microenvironment and leads to loss of therapeutic efficacy of checkpoint blockade, tumor antigen vaccination, and adoptive T-cell transfer immunotherapy approaches preclinically (11, 12). Although the above studies of tumor-intrinsic WNT/β-catenin signaling have

[1]Department of Medicine, The University of Chicago, Chicago, Illinois. [2]Center for Research Informatics, The University of Chicago, Chicago, Illinois. [3]Department of Pediatrics, The University of Chicago, Chicago, Illinois. [4]Department of Pathology, The University of Chicago, Chicago, Illinois.

Note: Supplementary data for this article are available at Clinical Cancer Research Online (http://clincancerres.aacrjournals.org/).

Current address for S. Spranger: Koch Institute for Integrative Cancer Research at MIT, Massachusetts Institute of Technology, Cambridge, Massachusetts.

Corresponding Author: Thomas F. Gajewski, The University of Chicago, 5841 South Maryland Avenue, MC2115, Chicago, IL 60637. Phone: 773-834-3096; Fax: 773-702-0963; E-mail: tgajewsk@medicine.bsd.uchicago.edu

doi: 10.1158/1078-0432.CCR-18-1942

Translational Relevance

Tumors can be categorized by gene expression based on the presence or absence of a T-cell-inflamed tumor microenvironment, and this phenotype correlates with response to immune-checkpoint blockade. WNT/β-catenin signaling in melanoma was the first tumor cell-intrinsic oncogenic signaling pathway linked to an immune exclusion phenotype. Here, we have profiled the correlation of WNT/β-catenin signaling and the T-cell-inflamed tumor microenvironment across The Cancer Genome Atlas. We have analyzed activated WNT/β-catenin signaling by somatic mutations, copy number alterations, gene expression, and reverse phase protein array showing a pan-cancer association of this signaling pathway with immune exclusion. These data highlight a high-priority unmet need for the development of selective Wnt/β-catenin pathway inhibitors as rational combination partners for immune-checkpoint blockade and identify tumor types for priority investigation.

been evaluated in the context of melanoma, the impact of this pathway in driving the non-T-cell-inflamed tumor microenvironment in other tumor types are increasingly being recognized. In syngeneic murine models of B16F10 melanoma, 4T1 mammary carcinoma, Neuro2A neuroblastoma, and Renca renal adenocarcinoma, blocking β-catenin pathway signaling via RNA interference resulted in influx of $CD8^+$ T cells and increase in IFNγ-associated gene targets (13). Subsequent combination with immunotherapy yielded complete regressions in the majority of treated animals. More broadly, roles for WNT/β-catenin signaling impacting on the immune system via development and function, active immune exclusion by tumor cells, and cancer immunosurveillance are being recognized and accepted across cancer types (14).

To investigate the influence of WNT/β-catenin signaling across cancers, we performed an integrative analysis of The Cancer Genome Atlas (TCGA) separating individual tumors by T-cell-inflamed status and identifying β-catenin pathway activation on three levels. We find that most tumor types within TCGA are enriched for activation of WNT/β-catenin signaling in non-T-cell-inflamed tumors. These observations suggest pharmacologic targeting of this pathway could have broad implications for improving immunotherapy efficacy.

Materials and Methods

TCGA cancer datasets

Level 3 gene expression data (release date February 4, 2015), level 4 somatic mutation data (release date January 28, 2016), and level 3 somatic copy number (CN) data (release date January 28, 2016) were downloaded for 31 solid tumor types from TCGA preprocessed by Broad's TCGA team (https://gdac.broadinstitute.org/). To make gene expression values comparable among cancer types, raw read counts mapped to gene features were processed by upper quartile normalization followed by log2 transformation across all samples. For mutation data, silent mutations were excluded from all analysis. For CN alterations, we focused on high-level changes including putative biallelic (or higher) CN gain (+2) or putative biallelic loss (−2) as defined in GISTIC2 data files entitled "all_thresholded_by_gene.txt" of each tumor type (15). The high-level somatic CN alterations (SCNAs) represent events where focal CN gain (or loss) are higher (or lower) than the maximum (or minimum) median arm-level CN gain (or loss), hence indicate more conservative thresholds and are less likely to be artifacts or false positives compared with low-level SCNAs given the purity and ploidy of tumor samples. Acute myeloid leukemia, diffuse large B-cell lymphoma, and thymoma were excluded because of high tumor cell-intrinsic immune cell transcripts. Skin cutaneous melanoma had both primary and metastatic samples available hence counted as two histologies, whereas the other 29 cancers had only primary tumors available. A total of 9,555 tumor samples and 742 normal samples were initially downloaded. After excluding the three tumor types, 9,244 tumors and 683 matched normal were included in the analysis.

Identification of non-T-cell-inflamed and T-cell-inflamed tumor groups

Using a defined T-cell-inflamed gene expression signature consisting of 160 genes ("concordant gene list," described in ref. 16), the tumor samples were categorized into three groups: non-T-cell-inflamed, T-cell-inflamed, and intermediate following previous protocols (16). In brief, a quantitative scoring system was developed to categorize tumors into three groups: non-T-cell-inflamed, T-cell-inflamed, and intermediate, based on the expression profile of the T-cell-inflamed gene expression signature. First, gene expression values were converted to a score $S_i = \mu_i \pm \beta_i\sigma_i$ ($i = 1,2, \ldots, n$), where μ and σ represent the mean and SD of the i th gene's expression across all samples, respectively. n is the total number of genes. β represents the distance between the i th gene's expression in a sample and its mean in the unit of SD (equivalent to a z-score). In this system, the threshold for non-T-cell-inflamed and T-cell-inflamed tumors was $\beta_0 = 0.1$. For each gene, if its coefficient $\beta_i > \beta_0$, then this gene is concluded as "upregulated" in this sample and assigned score as +1; likewise, if its coefficient $\beta_i < -\beta_0$, then this gene is concluded as "downregulated" in this sample and assigned score as −1; otherwise, this gene is concluded as `unchanged' and assigned score as 0. Next, the summation of the score across all 160 genes from the signature was computed to determine the group of a patient. As each gene score has values of −1, 0, or +1, the summation of all gene scores ranges from −160 (if all genes are downregulated) to +160 (if all genes are upregulated), where tumors of < −80 score summation were categorized as non-T-cell-inflamed, > +80 score summation as T-cell inflamed, and the rest as intermediate.

Differential gene expression detection and pathway activation prediction

Within each individual cancer, genes significantly differentially expressed between non-T-cell-inflamed and T-cell-inflamed tumor groups were identified by linear models for microarray and RNA-sequencing (RNA-seq) data (limma) voom algorithm with precision weights (17), filtered by FDR-adjusted $P < 0.05$, and fold change ≥ 1.5 or ≤ -1.5. Pathways significantly altered by the differentially expressed genes (DEG) were detected by IPA (Qiagen Inc.) using the curated Ingenuity Knowledge Base (accessed November 2015). Upstream transcriptional regulators

and their change of direction were predicted by the cumulative effect of target molecules upregulated or downregulated under condition (18). Those of overlap $P < 0.05$ (measuring the enrichment of target molecules in the dataset) were selected for further analysis. For each individual tumor sample, a β-catenin pathway activation score was calculated requiring at least 50% of the cancer-specific target molecules (Supplementary Table S1) to be upregulated (relative to its median expression across all samples from this individual cancer) in non-T-cell-inflamed tumor group relative to inflamed. For cancers where the total number of target molecules is less than 10, at least five molecules are required to be upregulated in order to determine a patient from this cancer to be activated; for cancers where the total number of target molecules is less than 5, all molecules must be upregulated in order to conclude that a patient is activated.

Estimation of stroma and immune cell enrichment from RNA-seq data

The relative enrichment of 64 stroma and immune cell types in tumor microenvironment was estimated by xCell (v1.1.0; ref. 19) from the bulk-tissue RNA-seq data. For each cell type, xCell assigns enrichment scores across all samples by integrating single-sample gene set enrichment analysis (ssGSEA) and deconvolution methods. All TCGA tumors were processed by xCell at once to compute per-sample stroma score and immune score, and then compared between β-catenin activated (activation score >0.5, high) and nonactivated samples (activation score ≤0.5, low) by nonparametric Mann–Whitney *U* test with FDR-correction for multiple comparisons.

Reverse phase protein array data analysis

Level 3 reverse phase protein array (RPPA) antibody-level protein abundance data (release date January 28, 2016; patch July 14, 2016) produced by The University of Texas MD Anderson Cancer Center were downloaded from TCGA preprocessed by Broad's TCGA team (https://gdac.broadinstitute.org/; accessed April 26, 2018). β-Catenin protein level was estimated using median-centered normalized values corresponding to antibody "β-catenin" from the data files without gene annotation. The gene-annotated RPPA data files were not used in this analysis due to potential gene symbol mismatch for β-catenin. Within each tumor type, a one-sided Pearson correlation (R function *cor.test*, alternative = "less") test was performed within each tumor type between β-catenin protein level and T-cell-inflamed gene expression from normalized RNA-seq data, followed by FDR-correction for multiple testing.

Statistical analysis

For analysis of contingency tables including comparison of sample frequency between groups activated by β-catenin pathway, Fisher exact test was used. Gene expression comparison between groups were performed using linear regression models implemented in limma voom. For multiple comparisons, *P*-value was adjusted using Benjamini–Hochberg FDR correction for multiple testing (20). Pearson correlation *r* was used for measuring statistical dependence between normalized and log2-transformed expression level of different genes. $P < 0.05$ was considered statistically significant and denoted as follows: *, $P < 0.05$; **, $P < 0.01$; ***, $P < 0.001$; ****, $P < 0.0001$. Statistical analysis was performed using R and Bioconductor.

Results

Solid tumor histologies can be segregated based on the degree of the T-cell-inflamed tumor microenvironment gene expression signature

Strong associations have been observed between the presence of T-cell-infiltration and/or a T-cell-inflamed gene expression signature and response to immune-checkpoint blockade (10, 21). These data imply that a non-T-cell-inflamed tumor microenvironment is associated with therapeutic resistance, and understanding the molecular basis of this phenotype should point towards candidate targets for expanding efficacy (10). To assess the landscape of the non-T-cell-inflamed tumor microenvironment across human cancers, we analyzed the RNA-seq data from 31 solid tumors contained within TCGA (Supplementary Table S2). We segregated samples into T-cell-inflamed, intermediate, or non-T-cell-inflamed using a T-cell-inflamed filtration score based on categorical definition (−1, 0, 1) of each gene from our previously defined 160-gene T-cell-inflamed expression signature (see Materials and Methods for further details; ref. 16). This gene expression signature shows a high level of correlation with a previously published immune cytolytic activity score used in other studies (Pearson $r = 0.83$; $P = 3.57e{-}09$; Supplementary Fig. S1; ref. 22).

Combining all cancer types within TCGA, 3,137/9,244 (33.9%) samples showed a non-T-cell-inflamed gene expression signature, with 2,946/9,244 (31.9%) scoring as intermediate and 3,161/9,244 (34.2%) displaying the T-cell-inflamed phenotype (Supplementary Fig. S2). Cancer types were ranked by the fraction of samples showing the non-T-cell-inflamed tumor microenvironment per tumor type (Fig. 1A). Paraganglioma, uveal melanoma, and adrenocortical tumors showed the highest frequency of non-T-cell-inflamed tumors, whereas lung adenocarcinoma, mesothelioma, and clear cell kidney cancer showed the lowest frequency of non-T-cell-inflamed samples. Relevant to clinical practice, this pattern approximates the activity of anti-PD-1/PD-L1 monotherapy in which little if any activity has been observed in uveal melanoma (23), whereas substantial clinical activity has been demonstrated in lung cancer, kidney cancer, and mesothelioma (24–26).

It was of interest to assess whether the T-cell-inflamed gene expression signature was a phenotype that was gained when comparing cancer tissue to normal tissue, or whether the non-T-cell-inflamed phenotype represented a loss of immune cell infiltration that is a component of normal tissue homeostasis. In most cases, loss of immune phenotype was observed in the malignant tissue. In tumor types of TCGA where adjacent normal tissue was available, non-T-cell-inflamed tumors generally showed a significantly lower T-cell-inflamed gene expression relative to normal tissue controls ($P = 1.10e{-}111$, two-sided Welch two sample *t* test) and the T-cell-inflamed tumors showed a significantly higher T-cell-inflamed gene expression relative to normal tissue ($P = 2.23e{-}106$). Within each individual tumor type, a similar pattern was observed for most cancers (Fig. 1B) with the exception of the three types of kidney cancer (chromophobe, clear cell, and renal papillary cell carcinoma), where those normal tissues showed a low T-cell-inflamed gene expression that was indistinguishable from that of non-T-cell-inflamed tumors ($P > 0.05$, ranges from 0.07–0.62). Although generally responsive to anti-PD-1 immunotherapy, the immunobiology of clear cell kidney cancer may

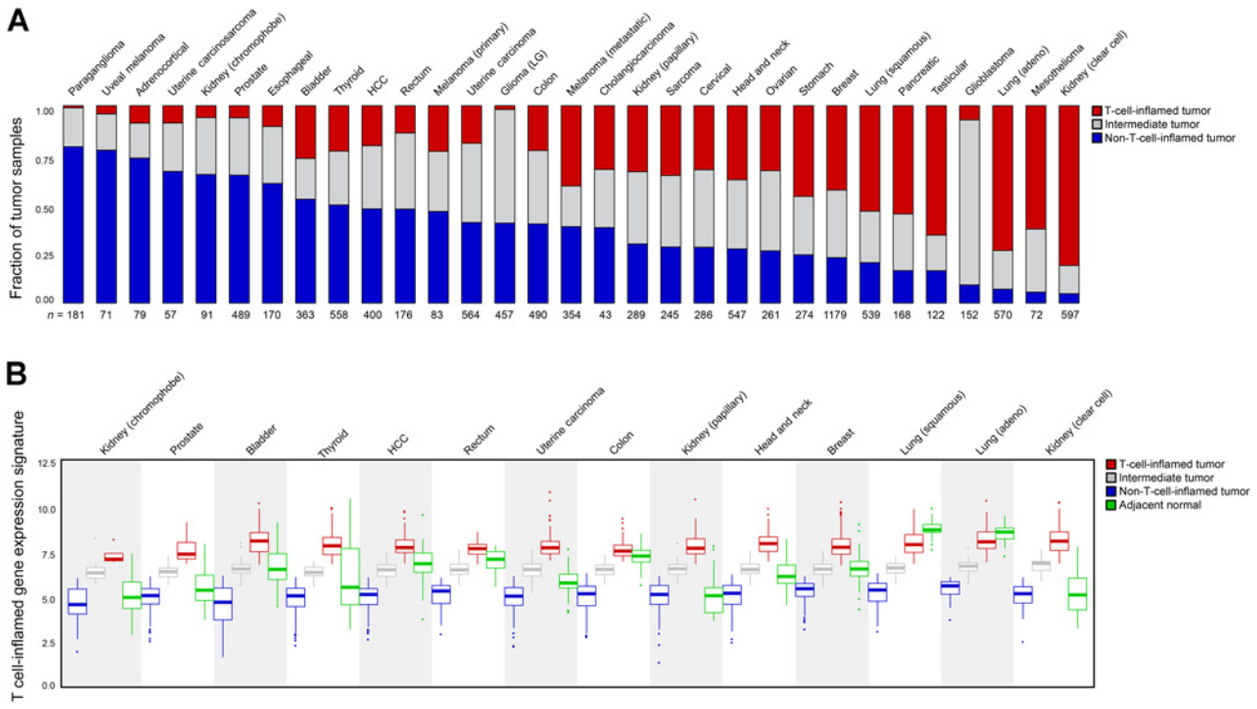

Figure 1.

Landscape of T-cell inflammation across 31 human solid tumors. **A,** The fraction of non-T-cell-inflamed (blue), intermediate (grey), and T-cell-inflamed (red) tumors in each cancer, sorted by the fraction of non-T-cell-inflamed tumor high to low, with the most non-inflamed cancer on the left (paraganglioma) and the most inflamed cancer on the right (kidney, clear cell). The number of samples in each cancer is shown on the x-axis. **B,** Distribution of T-cell-inflamed gene expression in non-T-cell-inflamed (blue), intermediate (grey), and T-cell-inflamed (red) tumors, as well as in normal samples (green). Cancers are shown on the x-axis in the same order as in **A,** and only 14 cancers with ≥10 normal samples are shown. The expression level of the T-cell-inflamed gene expression signature (defined as the average expression of genes from the signature in a sample) is shown on the y-axis. Each data point represents one tumor or normal sample adeno, adenocarcinoma; HCC, hepatocellular carcinoma; LG, low grade.

vary from other tumor types based on significant clinical activity despite low mutational density or neoantigen load (27), and the unexpected negative prognostic value of a higher $CD8^+$ T-cell density at baseline (28).

Having previously identified activated WNT/β-catenin signaling in 48% of non-T cell-inflamed metastatic melanoma samples (11), we investigated whether activation of this pathway was associated with the non-T cell-inflamed phenotype in other cancer histologies. β-Catenin pathway activation was addressed on three levels: somatic mutations or CN alterations in *CTNNB1* and other regulators predicted to yield pathway activation, expression of downstream target genes indicative of β-catenin signaling, and β-catenin protein levels as assessed by RPPA.

Somatic mutations of *CTNNB1* and upstream repressors are enriched in non-T-cell-inflamed tumors

To interrogate tumors for β-catenin pathway activation, nonsynonymous mutations (NSSM) across TCGA samples in the *CTNNB1*, *APC*, *APC2*, *AXIN1*, and *AXIN2* genes were identified and investigated for abundance within the non-T-cell-inflamed versus the T-cell-inflamed cohorts. This analysis was restricted to defined mutations predicted to mediate pathway activation. For *CTNNB1*, we defined relevant mutations as those affecting exon 3 (amino acid position 29–49) corresponding to the phosphorylation site by GSK3β which normally leads to proteolytic degradation of β-catenin (Fig. 2A). Across the aggregate TCGA cohort, we observed a statistically significant three-fold enrichment ($P < 0.0001$, two-sided Fisher exact test) of these mutations in non-T-cell-inflamed versus T-cell-inflamed tumors (Fig. 2B, black bars). Mutations were most commonly missense mutations effecting serine or threonine residues as previously published (29). For other β-catenin pathway genes, we included potential damaging mutations such as nonsynonymous or stopgain single nucleotide variants (SNV), variants that affect splicing site, and frameshift/non-frameshift small insertions and deletions (indels). We additionally analyzed high-level somatic CN gain for *CTNNB1* and CN loss for *APC*, *APC2*, *AXIN1*, and *AXIN2* (defined as ±2 in GISTIC2 data files; see Materials and Methods). Similarly to as activation mutations, *CTNNB1* CN gain occurred at a higher frequency in non-T-cell-inflamed tumors than T-cell-inflamed tumors (Fig. 2B, grey bars).

Across non-T-cell-inflamed tumors we observed 15.21% of samples as harboring mutations predicted to activate β-catenin signaling, SCNAs in pathway genes or both (Fig. 2C; Supplementary Fig. S3A and SB) as opposed to 10.06% in T cell-inflamed tumors (Supplementary Fig. S3C–S3E). These mutations and high-level SCNAs were predominately non-overlapping and were dominated by activating mutations in *CTNNB1* and damaging mutations in *APC*. Beyond exon 3, we identified 18 activation mutations located in exon 6, 7 or 8 based on known experimental evidence reported from the literature that occur on amino acid position 292 (30), 335 (31), 383 (30), and 387 (31)

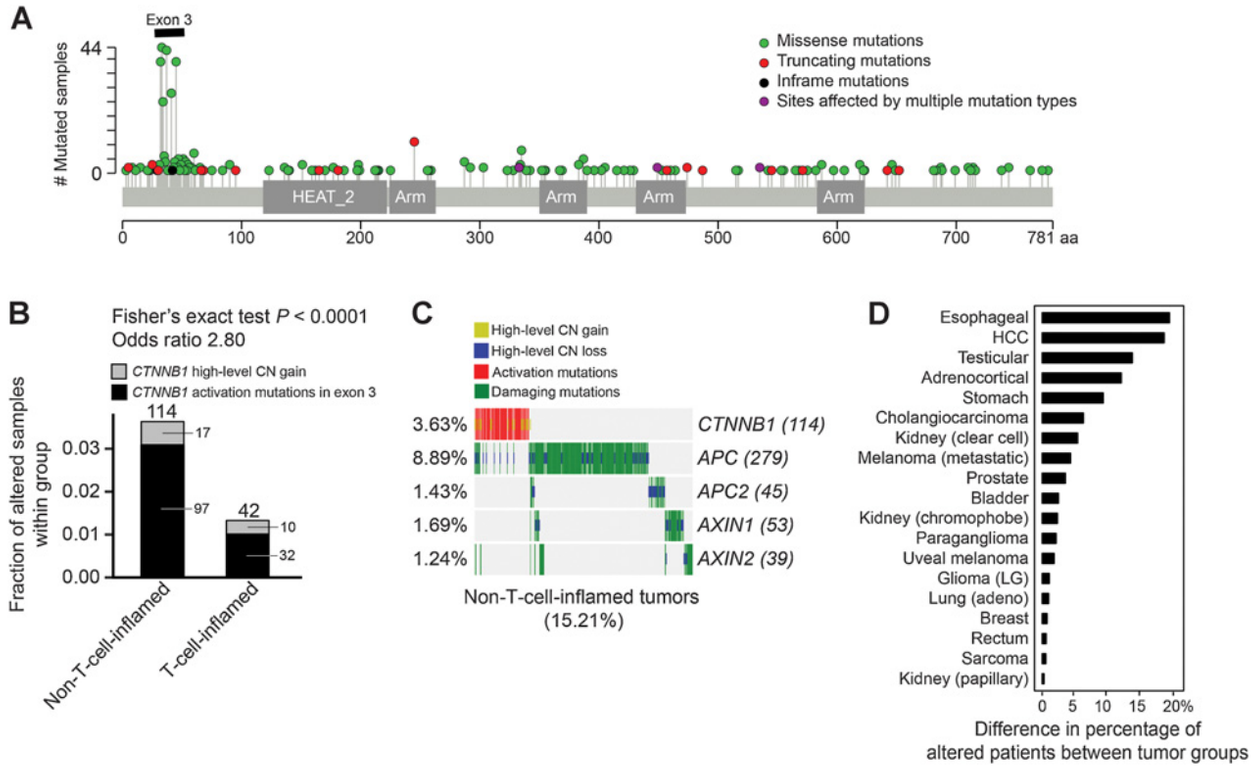

Figure 2.

Somatic mutation and high-level SCNA profile in β-catenin signaling in non-T-cell-inflamed and T-cell-inflamed tumor groups. **A,** Overview of potential coding somatic mutations in *CTNNB1* predicted to cause protein sequence changes. Each circle represents each amino acid (aa) change, with the height of the connection line representing the total number of samples carrying this mutation. Color of the circle represents mutation type, with missense mutations in green (nonsynonymous SNVs), truncating mutations in red (nonsense SNVs, frameshift deletions/insertions, splicing site variants), and in-frame mutations in blue (in-frame insertions/deletions/substitutions). Sites affected by multiple mutation types are colored in purple. Silent mutations (synonymous SNVs) are not shown. Protein domains are shown as dark grey boxes on the protein schema, HEAT_2 = HEAT repeats, and Arm = Armadillo/beta-catenin-like repeat as defined in Pfam database. **B,** Fraction of non-T-cell-inflamed and T-cell-inflamed tumors carrying β-catenin pathway activation mutations in exon 3 or high-level CN gain. The number above each bar represents the number of altered samples in each group. **C,** Landscape of activation mutations (exon 3) or high-level CN gain in *CTNNB1*, and damaging mutations or high-level CN loss in *APC, APC2, AXIN1*, and *AXIN2* across non-T-cell-inflamed tumors. The percentage of samples carrying mutations or SCNAs in each gene is presented on the left side, and the sample number is shown on the right side. Color represents predicted functional consequence of somatic mutations (red: activation; green: damaging) or SCNAs (gold: high-level CN gain; blue: high-level CN loss). **D,** Difference in the percentage of β-catenin-mutated or CN-altered patients between non-T-cell-inflamed and T-cell-inflamed tumor groups per cancer. Cancers are shown on the left side and sorted by percentage difference in patients carrying mutations between tumor groups (top to bottom: larger to smaller percentage differences). Nineteen cancers with a higher percentage of β-catenin-mutated patients in non-T-cell-inflamed tumor group relative to T-cell-inflamed group are shown. adeno, adenocarcinoma; HCC, hepatocellular carcinoma; LG, low grade.

(Supplementary Fig. S4). Consistent with those disrupting GSK3β-phosphorylation sites in exon 3, those additional mutations showed a strong anticorrelation with the T-cell-inflamed expression signature (10 in non-T-cell-inflamed, 7 in intermediate, and 1 in T-cell-inflamed group), potentially by reducing APC/AXIN1/AXIN2 binding or affecting ubiquitin-mediated protein degradation pathways. We acknowledge our analysis is likely an underestimated assessment of somatic mutations that drive β-catenin signaling activation, considering that mutations in genes other than *CTNNB1*, *APC, APC2*, *AXIN1*, and *AXIN2* may also be contributors (32, 33). Also, it is possible that SCNAs could be influenced by the presence of nontumor cells in the tissue. Across individual tumors, 19 cancer types showed a higher fraction of β-catenin pathway mutations, high-level SCNAs or both associated with non-T-cell-inflamed as compared with T-cell-inflamed tumors (Fig. 2D; Supplementary Fig. S5). Additionally, we compared the expression of the T-cell-inflamed gene expression signature with the fraction of β-catenin pathway altered samples (mutations or high-level SCNA changes in *CTNNB1, APC, APC2, AXIN1*, and *AXIN2*) per tumor type (Supplementary Fig. S6). We found a weak and statistically in-significant correlation across TCGA and within specific tumor types, suggesting that direct genomic activation of β-catenin by mutation or high-level SCNAs may not be the main driver of non-T-cell-inflamed phenotype. However, the results should be interpreted with caution considering the limited sample size for β-catenin pathway mutations or high-level SCNAs within each tumor type.

Activation of a β-catenin transcriptional program correlates with the non-T-cell-inflamed tumor microenvironment across tumor types

To describe the frequency of β-catenin pathway activation at the level of target gene expression, we identified genes significantly differentially expressed in non-T-cell-inflamed tumors relative to

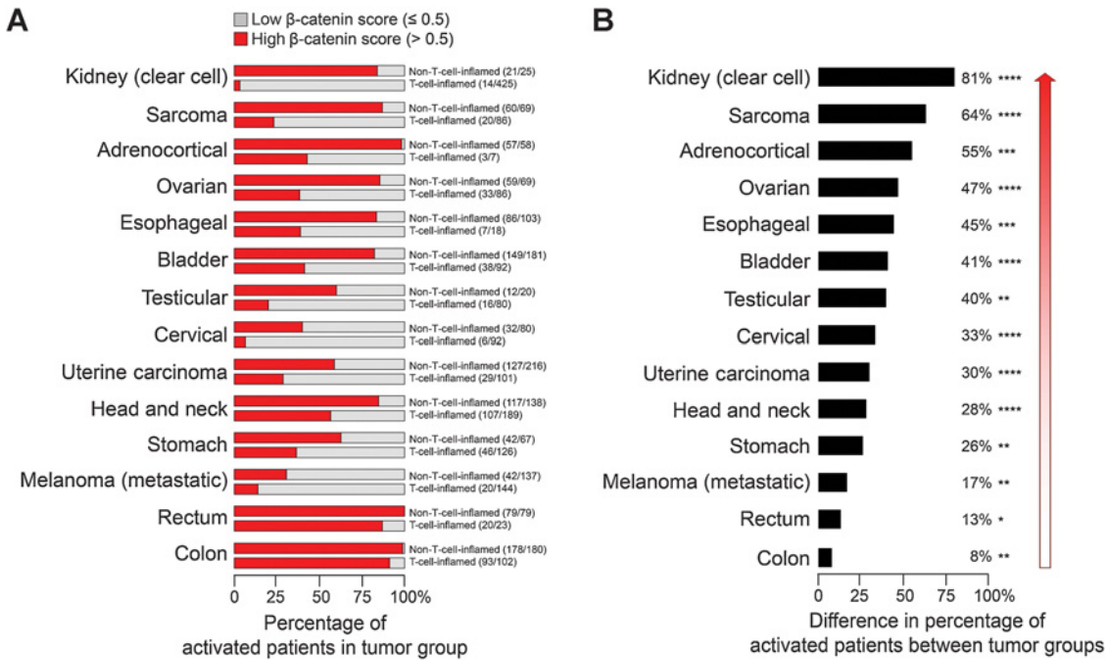

Figure 3.

β-Catenin activation in non-T-cell-inflamed and T-cell-inflamed tumor groups. Fourteen cancers with a significantly higher percentage of β-catenin-activated patients in non-T-cell-inflamed tumor group relative to T-cell-inflamed group and at least five target molecules are shown (also listed in Supplementary Table S1). **A,** The percentage of β-catenin-activated patients in each tumor group per cancer (β-catenin activation score >0.5), with the subset of tumors with β-catenin signaling activated and total number of tumor samples shown to the right side of each bar inside parentheses. **B,** Difference in the percentage of β-catenin-activated patients between non-T-cell-inflamed and T-cell-inflamed tumor groups per cancer. In both panels, cancers are shown to the left side and sorted by percentage difference in the activated patients between tumor groups (top to bottom: larger to smaller percentage differences). The significance of such difference was computed using Fisher exact test, two-sided. $P < 0.05$ was considered statistically significant, and significance is indicated by: ∗, $P < 0.05$; ∗∗, $P < 0.01$; ∗∗∗, $P < 0.001$; ∗∗∗∗, $P < 0.0001$, after FDR correction for multiple comparisons.

T-cell inflamed, and that overlapped with known downstream target molecules of CTNNB1 as upstream regulator from the curated Ingenuity Knowledge Base (Qiagen Inc.), yielding a β-catenin activation score for each patient. Downstream target molecules in this analysis are collated from the literature as being regulated by *CTNNB1* (18). We chose to accept a β-catenin activation score of >0.5 and scored individual samples as β-catenin activated or not activated. The percentage of activated samples in non-T-cell-inflamed versus T-cell inflamed was calculated for each tumor type. Of the 31 solid tumors from TCGA, 14 tumor types met the definition of WNT/β-catenin activation by pathway analysis and demonstrated a greater proportion of samples with β-catenin activation in the non-T-cell-inflamed versus T-cell inflamed (FDR-adjusted $P < 0.05$, two-sided Fisher exact test; Fig. 3A and B).

The individual target molecules identified by pathway analysis varied by tumor type though some were shared between tumors (Supplementary Table S1). A total of 201 β-catenin target molecules were identified in at least one tumor type with the top shared molecules in Supplementary Fig. S7, showing those shared by at least three tumor types for CTNNB1 as upstream regulator. Representative shared molecules across clear cell kidney, ovarian and stomach cancer include BMP7, WNT11, and TDGF1, which each demonstrates statistically significant inverse correlations with the T-cell-inflamed gene expression signature and upregulation of expression in non-T-cell-inflamed tumors (Supplementary Fig. S8). In particular, shared WNT molecules, such as WNT11, were found to be significantly upregulated in kidney renal papillary cell carcinoma, ovarian serous cystadenocarcinoma, stomach adenocarcinoma, and testicular germ cell tumors, suggesting that WNT11 may be a candidate therapeutic target in those cancer types (Supplementary Fig. S9).

To evaluate the potential contribution of stroma cells on the β-catenin pathway activation score, we analyzed all TCGA tumors at once to compute per-sample stroma score and immune score (19) from the RNA-seq data, and then compared the enrichment scores between β-catenin activated (activation score >0.5, high) and nonactivated samples (activation score ≤0.5, low; Supplementary Fig. S10). From the 14 tumor types where WNT/β-catenin activation by pathway analysis was observed, significant stroma score differences were detected in three tumor types (esophageal carcinoma, ovarian serous cystadenocarcinoma, testicular germ cell tumors) at FDR-adjusted $P < 0.05$ (Supplementary Fig. S10, top). Esophageal carcinoma showed reduced stroma score in the β-catenin–activated samples, however, the other two tumor types showed the opposite trend. In contrast, all 14 tumor types consistently showed a reduction in the immune score comparing the β-catenin activated to nonactivated samples, 13 of which reached the significance level of 0.05, with esophageal carcinoma at $P = 0.080$ (Supplementary Fig. S10, bottom). Taken together, those results do not appear to support a dominant role

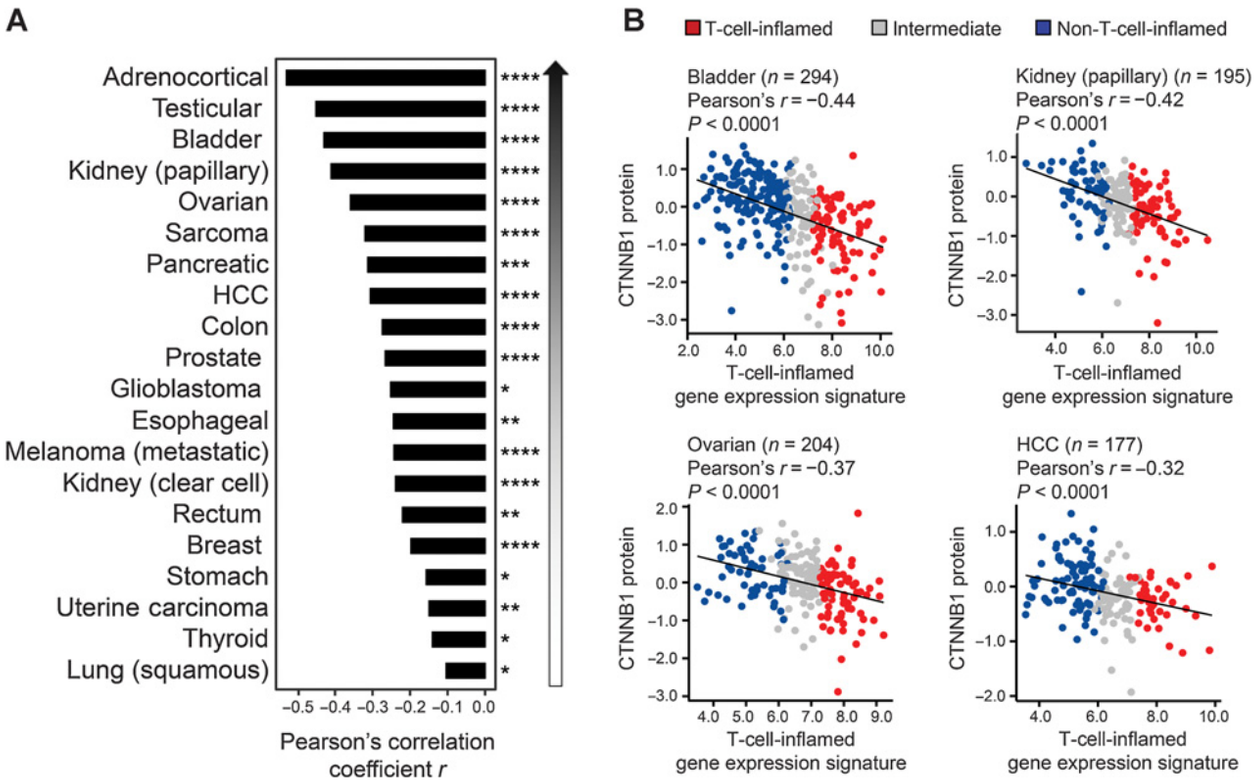

Figure 4.

Inverse correlation between β-catenin protein level and T-cell-inflamed gene expression. **A,** Pearson correlation per tumor type. Twenty cancers with significant inverse correlation are shown. **B,** Dot plots of β-catenin protein on y-axis and T-cell-inflamed gene expression on x-axis in bladder urothelial carcinoma, kidney (papillary), ovarian serous cystadenocarcinoma, and liver hepatocellular carcinoma shown with linear regression correlations using Pearson test. The significance of such difference was computed using Pearson correlation, one-sided test. $P < 0.05$ was considered statistically significant, and significance is indicated by: ∗, $P < 0.05$; ∗∗, $P < 0.01$; ∗∗∗, $P < 0.001$; ∗∗∗∗, $P < 0.0001$, after FDR correction for multiple comparisons. HCC, hepatocellular carcinoma.

for the contribution of stromal cells to β-catenin pathway activation across tumor types.

To assess whether somatic mutations of β-catenin pathway genes were associated with upregulated expression of downstream target genes, we overlapped samples carrying β-catenin pathway gene mutations or high-level SCNAs with samples with a high β-catenin activation score. From the 14 tumor types where WNT/β-catenin activation by pathway analysis was observed, we identified 291/348 (83.6%) as mutated or CN altered and activated in non-T-cell-inflamed as compared with 127/225 (56.4%) in T-cell-inflamed tumors (Supplementary Fig. S11). This demonstrates a significantly higher concordance between mutated samples and activated samples with a low level of T-cell inflammation ($P < 0.0001$; OR = 3.93, two-sided Fisher exact test).

β-Catenin protein level inversely correlates with the T-cell-inflamed tumor phenotype across tumor types

β-Catenin staining by IHC has previously been shown to inversely correlate with staining for $CD8^+$ T cells in melanoma and bladder cancer (11, 34). It was therefore of interest to analyze available RPPA data for β-catenin protein levels from TCGA and examine a potential inverse correlation with the T-cell-inflamed gene expression signature. Indeed, taking the aggregate data from all 31 TCGA tumors, a statistically significant inverse correlation was observed between β-catenin protein abundance and the T-cell-inflamed gene expression ($P < 0.0001$). Among individual cancer types, this inverse correlation was observed for 20 cancers subtypes at a significance level of FDR-adjusted $P < 0.05$ (Fig. 4A). Representative tumor types including bladder (Pearson $r = -0.44$; $P < 0.0001$), kidney renal papillary cell carcinoma (Pearson $r = -0.42$; $P < 0.0001$), ovarian serous cystadenocarcinoma (Pearson $r = -0.37$; $P < 0.0001$), and hepatocellular carcinoma (Pearson $r = -0.32$; $P < 0.0001$) are shown in Fig. 4B. All individual tumor types are included in Supplementary Fig. S12. Note that adrenocortical carcinoma showed the strongest anticorrelation (Pearson $r = -0.55$) but was not included in Fig. 4B due to relatively smaller sample size (46 samples with both RNA-seq and RPPA data available). Results for all analyses across all tumor types investigated above are shown as Supplementary Fig. S13.

Discussion

In our current analysis of the T-cell-inflamed versus non-T-cell-inflamed tumor microenvironment across the solid tumors as represented in TCGA, we observed that 33.9% of tumors were non-T-cell-inflamed, with most of these tumors showing lower immune gene expression compared with matched normal tissue.

Table 1. Summary of evidence for β-catenin signaling activation non-T-cell-inflamed tumors from the 31 cancer subtypes using three approaches

Cancer	Name	Joint evidence of activation in non-T-cell-inflamed tumors	Somatic mutation or high-level SCNA enrichment	Pathway gene expression activation	Higher CTNNB1 protein level
ACC	Adrenocortical	Tier 3	Y	Y	Y
BLCA	Bladder	Tier 3	Y	Y	Y
ESCA	Esophageal	Tier 3	Y	Y	Y
KIRC	Kidney (clear cell)	Tier 3	Y	Y	Y
SARC	Sarcoma	Tier 3	Y	Y	Y
SKCMmets	Melanoma (metastatic)	Tier 3	Y	Y	Y
READ	Rectum	Tier 3	Y	Y	Y
STAD	Stomach	Tier 3	Y	Y	Y
TGCT	Testicular	Tier 3	Y	Y	Y
BRCA	Breast	Tier 2	Y	N	Y
COAD	Colon	Tier 2	N	Y	Y
KIRP	Kidney (papillary)	Tier 2	Y	N	Y
LIHC	HCC	Tier 2	Y	N	Y
OV	Ovarian	Tier 2	N	Y	Y
PRAD	Prostate	Tier 2	Y	N	Y
UCEC	Uterine carcinoma	Tier 2	N	Y	Y
CESC	Cervical	Tier 1	N	Y	N
CHOL	Cholangiocarcinoma	Tier 1	Y	N	N
GBM	Glioblastoma	Tier 1	N	N	Y
HNSC	Head and neck	Tier 1	N	Y	N
KICH	Kidney (chromophobe)	Tier 1	Y	N	N
LGG	Glioma (LG)	Tier 1	Y	N	N
LUAD	Lung (adeno)	Tier 1	Y	N	N
LUSC	Lung (squamous)	Tier 1	N	N	Y
PAAD	Pancreatic	Tier 1	N	N	Y
PCPG	Paraganglioma	Tier 1	Y	N	N
THCA	Thyroid	Tier 1	N	N	Y
UVM	Uveal melanoma	Tier 1	Y	N	NE[a]
MESO	Mesothelioma	No tier	N[b]	N	N
SKCMprimary	Melanoma (primary)	No tier	NE[c]	N	N
UCS	Uterine carcinosarcoma	No tier	N	N	N

Abbreviations: adeno, adenocarcinoma; HCC, hepatocellular carcinoma; LG, low grade; N, lack of evidence; Y, presence of evidence.

[a]Uveal melanoma has a limited number of RPPA samples ($n = 12$), hence the correlation between T-cell-inflamed gene expression signature and its β-catenin protein level was nonevaluable (NE).

[b]Mesothelioma has GDAC-Firehose preprocessed level 3 CN data available; somatic mutation data were not available.

[c]Melanoma primary tumors do not have GDAC-Firehose preprocessed level 3 somatic mutation or CN data available, hence shown as nonevaluable (NE).

This observation suggests that the lack of T-cell–based tissue inflammation is a frequent occurrence in primary cancers and that loss of this biologic process could be a component of carcinogenesis. The development of the non-T-cell-inflamed tumor microenvironment therefore might be regulated by oncogenic events. Analysis of molecular evidence for WNT/β-catenin pathway activation as one potentially causal pathway revealed that as many as 28/31 (90%) of tumor types across TCGA showed an inverse correlation with a T-cell-inflamed gene expression signature. We inferred β-catenin pathway activation using three approaches: (i) somatic pathway mutations or high-level SCNAs, where 19 cancers showed a higher proportion of mutated samples in non-T-cell-inflamed group relative to inflamed; (ii) pathway target gene expression, where 14 cancers showed predicted β-catenin activation based on upregulation of known target molecules in non-T-cell-inflamed group relative to inflamed; (iii) β-catenin protein level by RPPA, where 20 cancers showed significant anticorrelation between β-catenin protein level and T-cell-inflamed gene expression. As a result, we categorized cancer subtypes into tier 1 to 3, with increasing support combining the three approaches (Table 1). In summary, we conclude that WNT/β-catenin pathway activation is frequently associated with poor spontaneous T-cell infiltration across most human cancers.

Of note, the three methods for analyzing WNT/β-catenin pathway activation did not give exactly concordant results. It is formally possible that some of the signal of both gene expression and β-catenin protein level may be derived from stromal cells in addition to cancer cells. Activating mutations in the β-catenin gene itself, as well as inactivating mutations in negative regulators of the β-catenin pathway, are likely restricted to the tumor cells. But all cell types theoretically have the potential to activate β-catenin signaling, including T cells and other immune cells. The non-T-cell-inflamed tumors that lack $CD8^+$ T cells also have few dendritic cells, so it is unlikely that increased β-catenin activation in those tumors is related to adaptive immunity. However, we observed limited contribution of stromal cells when comparing a stroma score between β-catenin pathway activated and nonactivated samples. Given that the most abundant cell type in these tumors is very likely the tumor cells themselves, these data support tumor-intrinsic β-catenin as a major correlate of the non-T-cell-inflamed tumor microenvironment. Future biomarker development to document the degree of β-catenin pathway activation should incorporate somatic mutations and SCNAs of the pathway coupled with IHC analysis of $CD8^+$ T cells along with stabilized β-catenin protein levels within tumor cells.

Identification of molecular factors associated with the non-T-cell-inflamed tumor microenvironment has important relevance for future development of combination immunotherapy regimens. Mechanistic studies using genetically-engineered mice have demonstrated that tumor cell-intrinsic β-catenin activation was sufficient to prevent spontaneous T-cell priming and infiltration into the tumor microenvironment, rendering those tumor-bearing mice resistant to combination checkpoint blockade therapy (11, 12). The molecular mechanism of this effect was mapped to defective recruitment and activation of Batf3-lineage dendritic cells, although additional mechanisms also may contribute. The lack of intratumoral Batf3 dendritic cells in β-catenin–expressing melanomas also rendered those tumors resistant to vaccination and adoptive T-cell transfer, arguing that this type of molecular aberration also could be relevant to other therapeutic modalities being explored clinically (11, 12).

The WNT/β-catenin pathway, therefore, should be a high priority molecular target for new drug development, in an effort to restore T-cell infiltration and potentially expand immunotherapy efficacy in the clinic. Several specific inhibitors have been developed and brought forward into early phase clinical trials; however, none have yet had sufficient monotherapy activity to advance further into registration trials (35). β-Catenin signaling is broadly utilized by many cell types, and on-target, off-tumor effects likely limit the potential therapeutic window. However, for cancer applications, most agents developed to date have likely been screened for the ability to slow cancer cell proliferation and/or induce cancer cell apoptosis. The immune evasive mechanisms of β-catenin activation, including suppression of chemokines and cytokine gene expression by tumor cells (11), may offer an opportunity to develop agents with more restricted activity that predominantly augment immunity while sparing other essential cellular functions.

In addition to WNT/β-catenin signaling as a major driver of immune exclusion, data are accumulating that other oncogenic events also can contribute to immune exclusion (36, 37). Loss of PTEN in melanoma has been associated with the non-T-cell-inflamed tumor microenvironment, and in that context inhibition of PI3K signaling synergized with immune-checkpoint blockade (38). PTEN/PI3K signaling has also been correlated with resistance to immunotherapy from a patient with uterine leiomyosarcoma who had previously had a complete response for 2 years prior to losing benefit from anti-PD-1 therapy (39). In bladder cancer, activating mutations in FGFR3, as well as molecular evidence for PPAR-γ activation, have been associated with the non-T-cell-inflamed tumor microenvironment (34). Inasmuch as FGFR inhibitors are currently in clinical development this may be the first pathway targeted to entertain the hypothesis that blockade of an immune-evasive oncogene pathway may improve immunotherapy efficacy in human cancer patients, as these agents will be combined with PD-1/PD-L1 blocking Abs as well (ClinicalTrials.gov Identifier: NCT02393248). Additionally, some tumors may possess a complicated interplay of multiple oncogenic events that synergize to mediate more potent immune exclusion, as has been reported for colorectal cancers showing activation of WNT/β-catenin, MYC, and RAS (33, 40, 41).

We acknowledge that our analysis may have some limitations. This current work was based on *in silico* analysis of TCGA. Although the T-cell-inflamed tumor microenvironment has been shown to predict response to multiple immunotherapies (as well as lack of response in non-T-cell-inflamed tumors; refs. 5, 10), the clinical outcomes of individual patients from TCGA were deliberately not encompassed in our analysis. Such a study is best performed prospectively in cohorts of patients receiving systemic therapy with the same immunotherapeutic agent, for example anti-PD-1. Our study is also limited in that the range of potential somatic genomic changes in the β-catenin pathway was restricted to point mutations and small insertions and deletions, as well as CN variants, whereas other types of genomic aberrations such as large-scale structural variants or gene fusions remain to be explored. Nonetheless, this set of data provides sufficient motivation to study baseline WNT/β-catenin pathway activation as a potential primary resistance pathway to checkpoint blockade in prospective clinical trials in defined patient cohorts.

Disclosure of Potential Conflicts of Interest

J.J. Luke reports receiving commercial research grants from Array, CheckMate, Evelo, and Palleon; reports receiving other commercial research support from AbbVie, Boston Biomedical, Bristol-Myers Squibb, Celldex, Compugen, Corvus, EMD Serono, Delcath, Five Prime, FLX Bio, Genentech, Immunocore, Incyte, Leap, MedImmune, Macrogenics, Novartis, Pharmacyclics, Merck, Tesaro, and Xencor; and is a consultant/advisory board member for TTC Oncology, 7 Hills, Actym, Alphamab Oncology, Array, BeneVir, Mavu, Tempest, Aduro, Astellas, AstraZeneca, Bayer, Bristol-Myers Squibb, Castle, CheckMate, Compugen EMD Serono, IDEAYA, Immunocore, Janssen, Jounce, Leap, Merck, NewLink, Novartis, ReleXion, Spring Bank, Syndax, Vividion, and WntRx. R.F. Sweis reports receiving commercial research grants from Bayer, speakers bureau honoraria from Bristol-Myers Squibb and Exelixis, and is a consultant/advisory board member for Bristol-Myers Squibb, Exelixis, AstraZeneca, Puma, and Eisai. S. Spranger reports receiving commercial research grants from Takeda and Exelecis, and is a consultant/advisory board member for Venn, Tango, Replimune, Takeda, Torque, Ribon, and Arcus. T.F. Gajewski reports receiving commercial research grants from Merck, Bristol-Myers Squibb, Seattle Genetics, Genentech, Ono, Evelo, Aduro, and Incyte; holds ownership interest (including patents) in Jounce, Evelo, Bristol-Myers Squibb, and Aduro; and is a consultant/advisory board member for Merck, Jounce, Aduro, Adaptimmune, FivePrime, and Fog Pharma. No potential conflicts of interest were disclosed by the other author.

Authors' Contributions

Conception and design: J.J. Luke, R. Bao, R.F. Sweis, S. Spranger, T.F. Gajewski
Development of methodology: J.J. Luke, R. Bao, R.F. Sweis, T.F. Gajewski
Acquisition of data (provided animals, acquired and managed patients, provided facilities, etc.): J.J. Luke, R. Bao, R.F. Sweis, T.F. Gajewski
Analysis and interpretation of data (e.g., statistical analysis, biostatistics, computational analysis): J.J. Luke, R. Bao, R.F. Sweis, T.F. Gajewski
Writing, review, and/or revision of the manuscript: J.J. Luke, R. Bao, R.F. Sweis, S. Spranger, T.F. Gajewski
Administrative, technical, or material support (i.e., reporting or organizing data, constructing databases): J.J. Luke, R. Bao
Study supervision: J.J. Luke, T.F. Gajewski

Acknowledgments

The bioinformatics analysis was performed on High-Performance Computing (HPC) clusters at Center for Research Informatics, Biological Sciences Division. The authors thank M. Jarsulic for technical assistance on the HPC clusters. J.J. Luke is supported by a U.S. Department of Defense Career Development Award (W81XWH-17-1-0265), the Arthur J. Schreiner Family Melanoma Research Fund, the J. Edward Mahoney Foundation Research Fund, the Brush Family Immunotherapy Research Fund and Buffet Fund for Cancer Immunotherapy with support from the Center for Research Informatics by the Biological Sciences Division at The University of Chicago, with additional support provided by the Institute for Translational Medicine/Clinical and Translational Award (NIH 5UL1TR002389-02), and The University of Chicago Comprehensive Cancer Center Support Grant (NIH P30CA014599). S. Spranger was a postdoctoral fellow of the Cancer Research Institute. T.F. Gajewski is supported by the American Cancer Society-Jules L. Plangere

Jr. Family Foundation Professorship in Cancer Immunotherapy, and R35 CA210098 from the NIH.

The costs of publication of this article were defrayed in part by the payment of page charges. This article must therefore be hereby marked *advertisement* in accordance with 18 U.S.C. Section 1734 solely to indicate this fact.

Received June 20, 2018; revised September 27, 2018; accepted January 7, 2019; published first January 11, 2019.

References

1. Topalian SL, Hodi FS, Brahmer JR, Gettinger SN, Smith DC, McDermott DF, et al. Safety, activity, and immune correlates of anti-PD-1 antibody in cancer. N Engl J Med 2012;366:2443–54.
2. Hodi FS, O'Day SJ, McDermott DF, Weber RW, Sosman JA, Haanen JB, et al. Improved survival with ipilimumab in patients with metastatic melanoma. N Engl J Med 2010;363:711–23.
3. Robert C, Schachter J, Long GV, Arance A, Grob JJ, Mortier L, et al. Pembrolizumab versus ipilimumab in advanced melanoma. N Engl J Med 2015;372:2521–32.
4. Larkin J, Chiarion-Sileni V, Gonzalez R, Grob JJ, Cowey CL, Lao CD, et al. Combined Nivolumab and Ipilimumab or Monotherapy in Untreated Melanoma. N Engl J Med 2015;373:23–34.
5. Harlin H, Meng Y, Peterson AC, Zha Y, Tretiakova M, Slingluff C, et al. Chemokine expression in melanoma metastases associated with CD8+ T-cell recruitment. Cancer Res 2009;69:3077–85.
6. Gajewski TF, Louahed J, Brichard VG. Gene signature in melanoma associated with clinical activity: a potential clue to unlock cancer immunotherapy. Cancer J 2010;16:399–403.
7. Gajewski TF, Schreiber H, Fu YX. Innate and adaptive immune cells in the tumor microenvironment. Nat Immunol 2013;14:1014–22.
8. Gajewski TF, Woo SR, Zha Y, Spaapen R, Zheng Y, Corrales L, et al. Cancer immunotherapy strategies based on overcoming barriers within the tumor microenvironment. Curr Opin Immunol 2013;25:268–76.
9. Ji RR, Chasalow SD, Wang L, Hamid O, Schmidt H, Cogswell J, et al. An immune-active tumor microenvironment favors clinical response to ipilimumab. Cancer Immunol Immunother 2012;61:1019–31.
10. Ayers M, Lunceford J, Nebozhyn M, Murphy E, Loboda A, Kaufman DR, et al. IFN-gamma-related mRNA profile predicts clinical response to PD-1 blockade. J Clin Invest 2017;127:2930–40.
11. Spranger S, Bao R, Gajewski TF. Melanoma-intrinsic beta-catenin signalling prevents anti-tumour immunity. Nature 2015;523:231–5.
12. Spranger S, Dai D, Horton B, Gajewski TF. Tumor-residing Batf3 dendritic cells are required for effector T cell trafficking and adoptive T cell therapy. Cancer Cell 2017;31:711–23.e4.
13. Ganesh S, Shui X, Craig KP, Park J, Wang W, Brown BD, et al. RNAi-mediated beta-catenin inhibition promotes T cell infiltration and antitumor activity in combination with immune checkpoint blockade. Mol Ther 2018;26:2567–79.
14. Galluzzi L, Spranger S, Fuchs E, Lopez-Soto A. WNT signaling in cancer immunosurveillance. Trends Cell Biol 2019;29:44–65.
15. Mermel CH, Schumacher SE, Hill B, Meyerson ML, Beroukhim R, Getz G. GISTIC2.0 facilitates sensitive and confident localization of the targets of focal somatic copy-number alteration in human cancers. Genome Biol 2011;12:R41.
16. Spranger S, Luke JJ, Bao R, Zha Y, Hernandez KM, Li Y, et al. Density of immunogenic antigens does not explain the presence or absence of the T-cell-inflamed tumor microenvironment in melanoma. Proc Natl Acad Sci U S A 2016;113:E7759–E68.
17. Law CW, Chen Y, Shi W, Smyth GK. voom: Precision weights unlock linear model analysis tools for RNA-seq read counts. Genome Biol 2014;15:R29.
18. Kramer A, Green J, Pollard J Jr, Tugendreich S. Causal analysis approaches in ingenuity pathway analysis. Bioinformatics 2014;30:523–30.
19. Aran D, Hu Z, Butte AJ. xCell: digitally portraying the tissue cellular heterogeneity landscape. Genome Biol 2017;18:220.
20. Benjamini Y, Drai D, Elmer G, Kafkafi N, Golani I. Controlling the false discovery rate in behavior genetics research. Behav Brain Res 2001;125:279–84.
21. Tumeh PC, Harview CL, Yearley JH, Shintaku IP, Taylor EJ, Robert L, et al. PD-1 blockade induces responses by inhibiting adaptive immune resistance. Nature 2014;515:568–71.
22. Rooney MS, Shukla SA, Wu CJ, Getz G, Hacohen N. Molecular and genetic properties of tumors associated with local immune cytolytic activity. Cell 2015;160:48–61.
23. Algazi AP, Tsai KK, Shoushtari AN, Munhoz RR, Eroglu Z, Piulats JM, et al. Clinical outcomes in metastatic uveal melanoma treated with PD-1 and PD-L1 antibodies. Cancer 2016;122:3344–53.
24. Brahmer J, Reckamp KL, Baas P, Crino L, Eberhardt WE, Poddubskaya E, et al. Nivolumab versus docetaxel in advanced squamous-cell non-small-cell lung cancer. N Engl J Med 2015;373:123–35.
25. Motzer RJ, Escudier B, McDermott DF, George S, Hammers HJ, Srinivas S, et al. Nivolumab versus everolimus in advanced renal-cell carcinoma. N Engl J Med 2015;373:1803–13.
26. Alley EW, Lopez J, Santoro A, Morosky A, Saraf S, Piperdi B, et al. Clinical safety and activity of pembrolizumab in patients with malignant pleural mesothelioma (KEYNOTE-028): preliminary results from a non-randomised, open-label, phase 1b trial. Lancet Oncol 2017;18:623–30.
27. Turajlic S, Litchfield K, Xu H, Rosenthal R, McGranahan N, Reading JL, et al. Insertion-and-deletion-derived tumour-specific neoantigens and the immunogenic phenotype: a pan-cancer analysis. Lancet Oncol 2017;18:1009–21.
28. Bromwich EJ, McArdle PA, Canna K, McMillan DC, McNicol AM, Brown M, et al. The relationship between T-lymphocyte infiltration, stage, tumour grade and survival in patients undergoing curative surgery for renal cell cancer. Br J Cancer 2003;89:1906–8.
29. Provost E, Yamamoto Y, Lizardi I, Stern J, D'Aquila TG, Gaynor RB, et al. Functional correlates of mutations in beta-catenin exon 3 phosphorylation sites. J Biol Chem 2003;278:31781–9.
30. von Kries JP, Winbeck G, Asbrand C, Schwarz-Romond T, Sochnikova N, Dell'Oro A, et al. Hot spots in beta-catenin for interactions with LEF-1, conductin and APC. Nat Struct Biol 2000;7:800–7.
31. Pilati C, Letouze E, Nault JC, Imbeaud S, Boulai A, Calderaro J, et al. Genomic profiling of hepatocellular adenomas reveals recurrent FRK-activating mutations and the mechanisms of malignant transformation. Cancer Cell 2014;25:428–41.
32. Giannakis M, Mu XJ, Shukla SA, Qian ZR, Cohen O, Nishihara R, et al. Genomic Correlates of Immune-cell infiltrates in colorectal carcinoma. Cell Rep 2016;15:857–65.
33. Grasso CS, Giannakis M, Wells DK, Hamada T, Mu XJ, Quist M, et al. Genetic mechanisms of immune evasion in colorectal cancer. Cancer Discov 2018;8:730–49.
34. Sweis RF, Spranger S, Bao R, Paner GP, Stadler WM, Steinberg G, et al. Molecular drivers of the non-T-cell-inflamed tumor microenvironment in urothelial bladder cancer. Cancer Immunol Res 2016;4:563–8.
35. Voronkov A, Krauss S. Wnt/beta-catenin signaling and small molecule inhibitors. Curr Pharm Des 2013;19:634–64.
36. Gajewski TF, Corrales L, Williams J, Horton B, Sivan A, Spranger S. Cancer immunotherapy targets based on understanding the T cell-inflamed versus non-T cell-inflamed tumor microenvironment. Adv Exp Med Biol 2017;1036:19–31.
37. Spranger S, Gajewski TF. Impact of oncogenic pathways on evasion of antitumour immune responses. Nat Rev Cancer 2018;18:139–47.
38. Peng W, Chen JQ, Liu C, Malu S, Creasy C, Tetzlaff MT, et al. Loss of PTEN promotes resistance to T cell-mediated immunotherapy. Cancer Discov 2016;6:202–16.
39. George S, Miao D, Demetri GD, Adeegbe D, Rodig SJ, Shukla S, et al. Loss of PTEN is associated with resistance to anti-PD-1 checkpoint blockade therapy in metastatic uterine leiomyosarcoma. Immunity 2017;46:197–204.
40. Guinney J, Dienstmann R, Wang X, de Reynies A, Schlicker A, Soneson C, et al. The consensus molecular subtypes of colorectal cancer. Nat Med 2015;21:1350–6.
41. Lal N, White BS, Goussous G, Pickles O, Mason MJ, Beggs AD, et al. KRAS Mutation and consensus molecular subtypes 2 and 3 Are Independently associated with reduced immune infiltration and reactivity in colorectal cancer. Clin Cancer Res 2018;24:224–33.